The Journal of Korean Vacuum Science & Technology
Vol. 2, No. 2, October 1998, pp. 85~91

Reaction process in electrochromism of tungsten oxide thin films

Ilsin An, Chang-Hyo Lee and Won-Taeg Lim

Department of Physics, Hanyang University, Ansan 425-791 Korea
(Received July 3, 1998)

Abstract – The electrochromic behaviors of dc-magnetron sputtered tungsten oxide thin films were investigated during coloration and bleach cycles using *in situ* real-time spectroscopic ellipsometry. Effective medium approximation and least-squares regression analyses were employed to investigate the electrochromic process. The optical properties of the tungsten oxide film were analyzed using the oscillator model and the evolution of the parameters were shown. Based on the optical observation, we have characterized the kinetics of the process using a reaction-limited model. In these analyses, we found that two different reaction rates were associated with the process. We ascribe this behavior to the microstructure of thin films.

I. Introduction

There have been many studies of the electrochromic behavior of WO_3 films for a variety of technological applications such as display devices and energy efficiency windows [1, 2]. Electrochromism (EC) occurs in many organic materials as well as in transition metal oxides. Among them WO_3 is the most widely studied material. Recently EC in many materials are reviewed by Granqvist [3] and reminisced by Deb who originally triggered this research [4].

WO_3 is optically transparent in the visible region and it turns blue when immersed in an electrolyte containing alkaline ions and subjected to an electric field. This process is reversible by switching the polarity of electric field. However, there have been many models proposed to account for the electrochromism in WO_3. Among them double charge injection [5], small polaron absorption [6], and free electron absorption [7] are prominent models. Recently, a two-phase model was proposed in which colored WO_3 consist of regions of metallic M_xWO_3 (here M_x alkaline ion) and insulating WO_3 with absorption based on an effective medium theory [8]. Also, Goldner *et al.* demonstrated the success of the free carrier model using near IR spectra of polycrystalline film [9]. They injected the same amount of charge into thin and thick WO_3 films and found that the absorptivity and reflectivity modulation were greater in the thin sample. From the thickness dependence of the optical properties they concluded that the free carrier density plays an important role in EC. However, the free carrier model alone cannot account for the spectrum near the UV region where the absorption peak of bleached WO_3 still remains upon coloration.

In this study, we employed real-time spectroscopic ellipsometry (SE) along with potentiostat measurement in order to investigate the evolution of the optical properties of WO_3 during EC process. In the analysis, we adopted the two-phase model and derived information on kinetics in coloration, which was based on reaction-limited process.

II. Experimental

Since electrochromism requires a device structure, WO_3 thin films need to be deposited on a conducting electrode. Thus, for the real-time SE

experiment, opaque chromium (Cr) films were sputtered onto Corning 7059 glass substrates. A low Ar gas pressure of 1.5 mTorr was used to ensure smooth and dense Cr films. We found 6 Å rms surface roughness from atomic force microscopy (AFM) measurement. The smooth Cr surface enables us to use a simple optical model of WO_3 on Cr without adding an additional interface layer. WO_3 films were prepared by a reactive dc magnetron sputtering technique. A pure tungsten target was sputtered in ~10 mTorr oxygen ambient at room temperature. Typical thickness of WO_3 film used in the studies was in the range of <200 Å. This range of thickness guarantees fast ion diffusion into the film so that we could observe a dominant reaction-limited process. The structure for the EC device is shown in Fig. 1 along with experimental setup for *in situ* real-time studies.

For voltage application and current measurements, a standard three-electrodes potentiostat was employed. The WO_3 device formed the working electrode in an electrochemical cell containing fused silica windows for optical access. The ellipsometer used in this study was a rotating polarizer type with a multichannel detection system [10]. This novel detection system allows the instrument to obtain continuous spectra consisting of ~100 data points from 1.5 to 4.3 eV with acquisition and repetition times as short as a fraction of second. Potentials versus reference electrode of 0.4 V and −0.3 V were applied to the working electrode for the bleach and color cycles, respectively. These values were chosen to avoid the breakdown of reversible EC behavior of the film, which occurred around 0.7 V in our samples. Before real-time SE measurements, these potential steps were applied repeatedly for many cycles to increase the stability of the film. The electrolytes were 0.1 M H_2SO_4 in H_2O and lithium perchlorate in organic propylene carbonate with a Pt wire used as a counter electrode and saturated calomel electrode (SCE) as a reference.

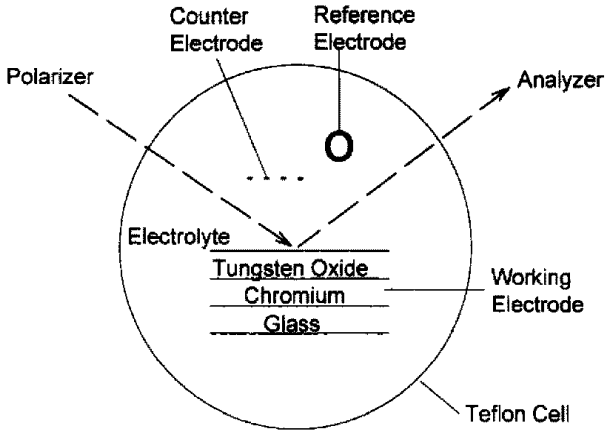

Fig. 1. Schematics of chemical cell used for this study.

III. Results and Discussion

Fig. 2 shows the evolution of the ellipsometric parameter, Ψ, for 120 s during a complete color-bleach cycle upon the applications of step-like potentials to 190 Å films in two different ion sources. Specifically, −0.3 V and 0.4 V vs. SCE were applied repeatedly to the working electrode for a period of 60 s and each pair of ellipsometry spectra $\{\Psi(eV), \Delta(eV)\}$ were collected every second with a pure data acquisition time of 128 ms. For clear demonstration, the single energy data at 2.0 eV were selected from 300 pairs of spectra over 1.5-4.3 eV. The high energy truncation was caused by strong UV absorption in aqueous electrolyte. The conventional ellipsometry angles, (Ψ, Δ) can be defined by the complex reflectivity ratio, $r_p/r_s = \tan\Psi\exp(i\Delta)$, where $r_{p(s)}$ is a parallel (perpendicular) component of the Fresnel reflection coefficients.

By simple inspection of Fig. 2, we can easily tell that the EC process is reversible and the process is faster in Li^+ environment than in H^+. The latter phenomenon can not be understood with a diffusion model. Also the bleach process is much faster than the coloration. Detailed information can be obtained from further analysis.

The optical properties of WO_3 film at any

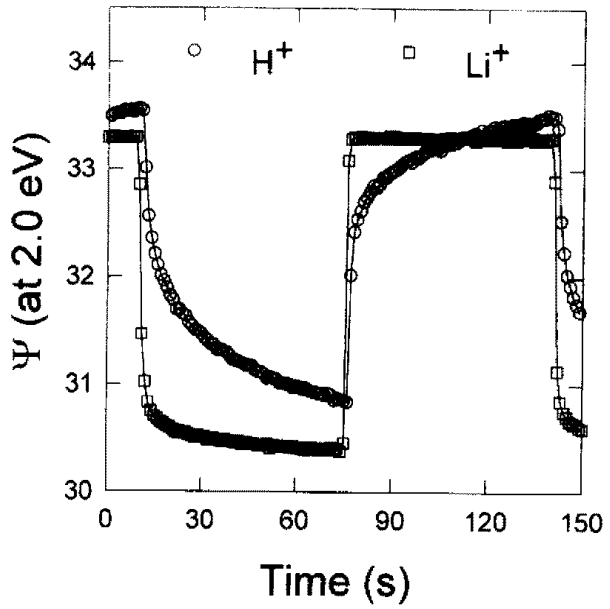

Fig. 2. Evolution of ellipsometry parameter (Ψ at 2.5 eV) during a complete cycle of coloration and bleach in two different ionic solutions (open circles: in hydrogen ion, open squares: in lithium ion). Step-like voltage of −0.3 V and 0.4 V vs. SCE were applied for a period of 60 s.

electrochromic stage can be deduced from mathematical inversion of each ellipsometry spectra under the assumption that the device maintains the electrolyte/film/Cr structure. The dielectric functions, $\varepsilon=\varepsilon_1+i\varepsilon_2$, of WO_3 at the beginning and the end of coloration stage are shown in Fig. 3. The filled circles depict the dielectric function of the WO_3 sample under 60 s into coloration (−0.3 V vs. SCE) in aqueous electrolyte, i.e., dielectric function of H_xWO_3. As we can see from the imaginary part of dielectric function, ε_2, of bleached WO_3 in Fig. 3, the bleached film is transparent to visible light and absorbing in the near UV region (i.e., rise of ε_2 above 3.5 eV). Meanwhile, the colored film shows two distinctive behaviors; one is the development of absorption in the near IR region, i.e., non-zero values of ε_2 between 1.5 eV and 3.5 eV and the other is small reduction in absorption in the near UV region, where the ε_2 peak still remains after coloration. This gives us the idea of employing the effective medium approximation (EMA) by which the optical properties of the colored film can possess those of the original.

Fig. 4 shows the optical trajectory taken during 60 s coloration process (open circles) in 190 Å film. In a diffusion model the optical trajectory is calculated using layer-by-layer progress of coloration from surface (solid lines) but in a reaction

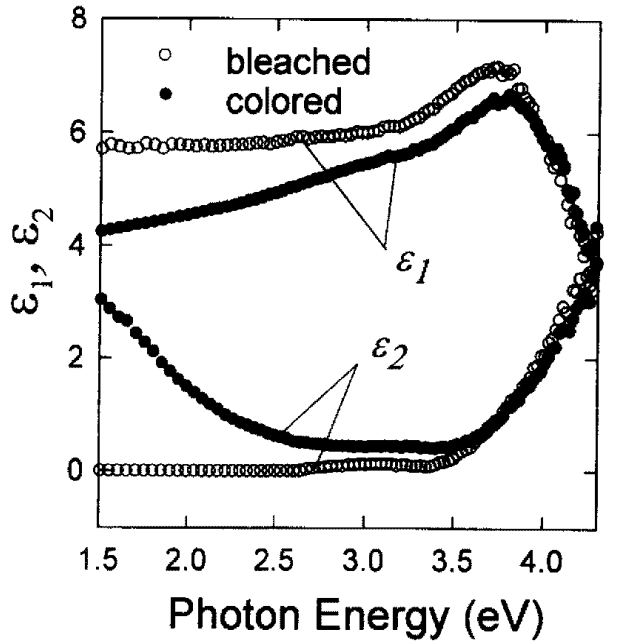

Fig. 3. Dielectric functions of colored and bleached states measured in aqueous electrolyte.

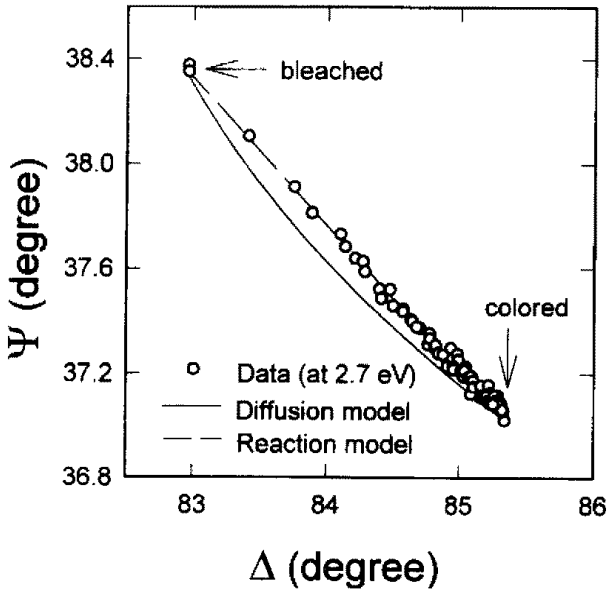

Fig. 4. Optical trajectory measured from the beginning to the end of color cycle (open circles). Broken line is a fit to a reaction model and solid line is a fit to a diffusion model.

model progressive change throughout the entire thickness of the WO_3 film is assumed (broken line). From this analysis, we find that the coloration is a dominant reaction process in our thin film and similar result was obtained for the bleach process. In thick films, however, both reaction and diffusion processes will compete each other. The diffusivity of hydrogen ion in WO_3 film lies between $10^{-7}cm^2/s$ and $10^{-11}cm^2/s$ depending on preparation methods and conditions [11]. Considering the relatively high diffusivity of hydrogen ion in WO_3 and the film thickness of 190 Å, the diffusion-limited phenomenon is not observable in the time scale of 60 s. Moreover, as we have already noticed in Fig. 2, the optical change with Li^+ is much faster than H^+ despite much lower diffusivity of Li^+ in WO_3 film [11]. At this moment, the possible explanation for this is that the mechanism of diffusion is different from that of reaction and the reaction between Li^+ and WO_3 is faster than that between H^+ and WO_3. In the following analyses, we used the data obtained with H^+ due to the well-known optical properties of electrolyte.

From these observations we applied two different approaches to interpret the optical properties of WO_3 at any intermediate stage between bleached and colored states. The first approach was using EMA with a free electron model expressed by following Drude oscillator.

$$\varepsilon_1 = \varepsilon_0 - [\omega_p^2/(\omega^2+\Gamma^2)] \quad (1)$$

$$\varepsilon_2 = (\Gamma/\omega)[\omega_p^2+\Gamma^2)] \quad (2)$$

These equations have three unknown free parameters to be determined in the fitting process. ε_0 is the bound carrier contribution to ε_1, ω_p is the plasma frequency of the free carriers, and Γ is a damping parameter.

The free electron contribution was observed in many previous researches near infrared [9, 12]. However, in our case the idea is based on the feature of the optical properties in near IR and visible range along with the increase in conductivity upon coloration. Furthermore, we expect that the real-time measurements will provide the information on trend. If we focus on the dielectric function of the colored film in Fig. 3, the dispersions of ε_1 and ε_2 below 3.5 eV show typical metallic properties. Thus, in this model, it is assumed that the optical properties of WO_3 in any electrochromic stage can be expressed as a mixture of the Drude free electron contribution and the original dielectric properties of WO_3. The Bruggeman EMA was used to calculate the optical properties of the mixture [13]. Fig. 5 shows the evolution of two of these parameters during the coloration cycle. As the plasma frequency $\omega_p \propto n^{1/2}$, where n is the free carrier density, we can conclude that the blue color is related to the development of free carrier absorption in the near IR region. Also damping parameter, Γ, is decreasing with coloration as it would be. The trends of both parameters support

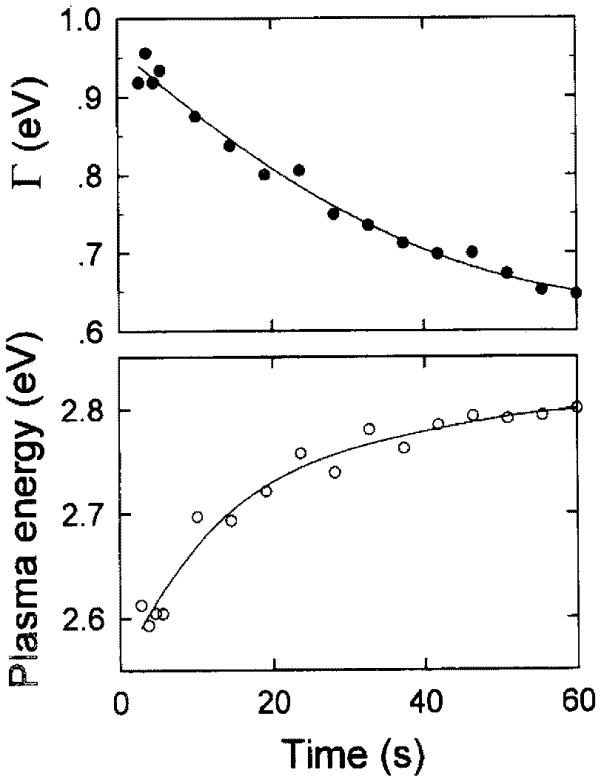

Fig. 5. Evolution of the Drude parameters: (top) damping parameter, (bottom) plasma energy.

the increase in conductivity of the film upon coloration and the values of both parameters are reasonable compared to those of typical metal and those of reported one [9].

Although the results are satisfactory with this analysis, we do not want to stress much on the Drude model because the metallic behavior always appears in the high energy shoulder of the optical function showing band transition, where the Lorentz oscillator model is appropriate [14]. The trends of ω_p and Γ obtained with the Lorentz oscillator were same as those shown in Fig. 5. With the limited spectral range of our detection system, either oscillator model was fine to deduce the temporal information on coloration as long as the quality of fit was acceptable. Currently we developed real-time SE with variable spectral range and detailed study regarding the optical properties near IR is in progress for future publication.

In the second method, we used two dielectric functions, those corresponding to the bleached and colored stages, to express any spectrum between the two extreme. This method has an advantage over the first one. That is, we do not need to know the detailed optical information on colored film. Thus, the only parameter to be determined in the analysis is the relative volume fraction of colored portion in WO_3 material, i.e., the optical amount of H_xWO_3.

The upper panel in Fig. 6 shows the evolution of the relative volume fractions obtained from both models during coloration. In this figure, the scale for each coordinate was intentionally adjusted for better comparison. We can notice that both methods are fine to extract the temporal information on the process. For comparison the total charges involved in process were shown in the bottom panel of Fig. 6. Although the resemblance to the upper panel is what we expected, this figure can not be obtained without considering leakage current. There was unintentional

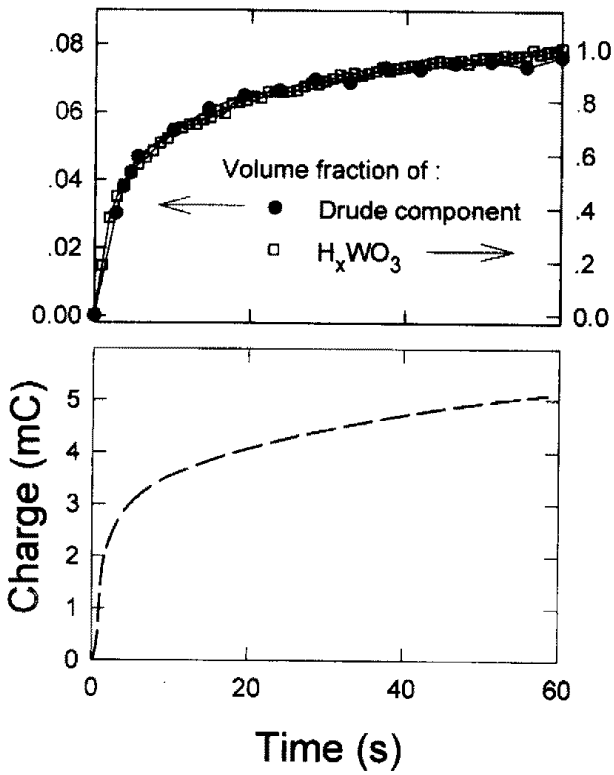

Fig. 6. (top) Evolution of the volume fractions obtained from two different models: Drude component (filled circles) and relative volume fraction of H_xWO_3 (open squares), (bottom) evolution of total charge.

internal short-circuit current [15] and it was estimated 0.25 mA/cm^2 for our samples. From the total charge involved in the coloration, we could estimate x=0.42 for H_xWO_3. This value is about 5 times larger than the volume fraction of Drude component in colored film. This means that most of the original optical properties of WO_3 remain after intercalation of hydrogen ion, which is expected from Fig. 3.

For further analysis of these results, we employed a reaction model in which the evolution of the volume fraction of colored portion, f(t), can be approximated by a single reaction rate α.

$$f(t) \approx 1 - exp(-\alpha t). \quad (3)$$

This equation represents the following process.

$$xH^+ + xe^- + WO_3 \rightarrow H_xWO_3. \quad (4)$$

However, the fits with Eq. (3) were poor for both coloration and bleach processes (broken lines in

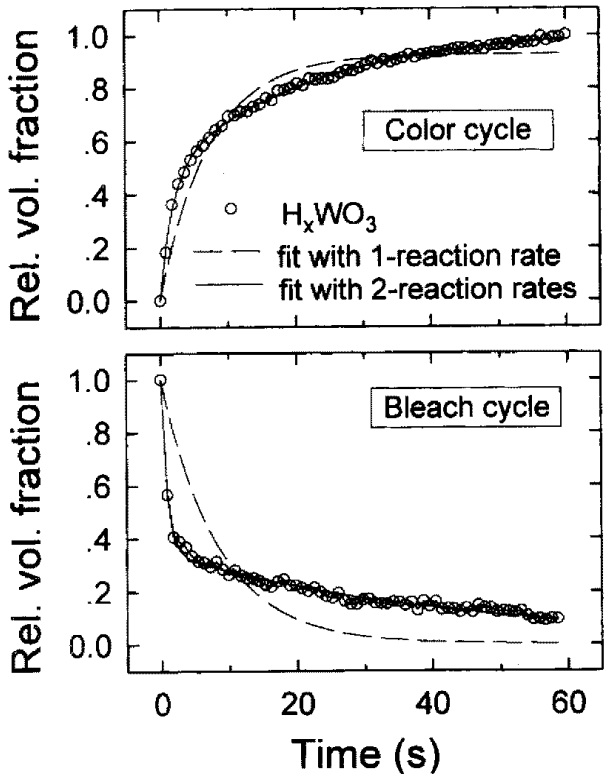

Fig. 7. Evolution of the volume fraction during color and bleach cycles. Fit to the reaction models with a single reaction rate (broken lines) and double reaction rates (solid lines).

Fig. 7). As the morphology of thin film shows grain structure in general, we assumed the reaction process at internal surface would be different from that inside grain. With this idea we tried two different reaction processes expressed by the following equation.

$$f(t) \approx 1 - f_1 \exp(-\alpha_1 t) - f_2 \exp(-\alpha_2 t), \quad (5)$$

where f_1 and f_2 are assumed to be the effective volume fractions of internal surface and bulk-like grain. And α_1 and α_2 are reaction rates for the corresponding sites. With this model almost perfect fits were obtained for both coloration and bleach processes (solid lines in Fig. 7). As we mentioned, we ascribe this behavior to the morphology of the film which has both dense and less dense sites related to columnar growth.

The deduced reaction rates and the volume fractions are shown in Table 1. As expected, one site shows about one order higher reaction rate than the other for coloration process. The bleach process is much faster in general and the relative volume fraction of fast and slow reaction site varies. The bleach process is even faster with Li ion, as we can see in Fig. 2. This might be related to the difference in activation energies in the reversible process. We also expect that the difference in environment such as conductivity of the film can play a role.

Table 1. Reaction rates (α) and volume fractions (f)

	α_1	f_1	α_2	f_2
coloration	0.53	0.48	0.045	0.52
bleach	1.13	0.65	0.023	0.35

IV. Conclusion

The coloration and bleach processes in thin WO_3 film were investigated using in situ real-time spectroscopic ellipsometry. Optical analysis showed that they were reaction-limited processes and the oscillator model and effective medium approximation were used for the analysis. The trends of the oscillator parameters supported the idea that the electron density is responsible for the near IR absorption. Also the reaction process was understood from the evolution of relative volume fraction of the colored portion of film. From the temporal information of the reaction, we found that two reaction rates were associated with the process and we ascribed this to the morphology of thin film.

Acknowledgment

This work was supported by KOSEF (971-0210-042-2). Authors thank to Prof. R. W. Collins at The Pennsylvania State University for comments on the original version of the manuscript.

References

1. D. K. Benson and H. M. Branz, Solar Energy Materials and Solar Cells, **39**, 203 (1995).
2. N. R. Lynam and A. A. Agrawal, *Large-Area Chromogenics: Materials and Devices for Transmittance Control* Vol. IS 4, eds. C. M. Lampert and C. G. Granqvist, SPIE Optical Engineering Press, 45 (1988).
3. C. G. Granqvist, *Handbook of Inorganic Electrochromic Materials*, Elsevier (1995).
4. S. K. Deb, Solar Energy Materials and Solar Cells **39**, 191 (1995).
5. B. W. Faughnan and R. S. Crandall, *Topics in Applied Physics*: Display Devices Vol. 40, ed. J. I. Pankove, Springer, 181 (1980).
6. O. F. Schimir, V. Wittwer, G. Baur, and G. Brandt, J. Electrochem. Soc. **124**, 749 (1977).
7. J. Zhang and K. Colbow, Appl. Phys. Lett. **58**, 1013 (1991).
8. H. S. Witham, P. Chindaudom, I. An, R. W. Collins, R. Messier, and K. Vedam, J. Vac. Sci. Technol. A **11**, 1881 (1993).
9. R. B. Goldner, P. Norton, K. Wong, G. Foley, E. L. Goldner, G. Seward, and R. Chapman, Appl. Phys. Lett. **47**, 536 (1985).
10. I. An and R. W. Collins, Rev. Sci. Instrum. **62**, 1904 (1991).
11. Chap. 6 in reference 3.
12. D. H. Mendelsohn and R. B. Goldner, J. Electrochem. Soc. **131**, 857 (1984).
13. G. A. Niklassen, C. G. Granqvist, and O. Hunderi, Appl. Opt. **20**, 26 (1981).
14. F. Wooten, Optical Properties of Solids, Academic Press, (1972).
15. C. Bechinger, J. N. Bullok, J.-G. Zhang, C. E. Tracy, D. K. Benson, S. K. Deb, and H. M. Branz, J. Appl. Phys. **80**, 1226 (1996).
16. R. Messier, A. P. Giri, and R. A. Roy, J. Vac. Sci. Technol. A **2**, 500 (1984).